Dynamic characteristics of an all-optical inverter based on polarization switching in long-wavelength VCSELs

A. Quirce, J. R. Cuesta, A. Hurtado, K. Schires, A. Valle, L. Pesquera, I. D. Henning,

and M. J. Adams

***Abstract*—An all-optical inverter using Polarization Switching (PS) of a long-wavelength single-mode vertical-cavity surface-emitting laser (VCSEL) is experimentally demonstrated. PS appears when linearly polarized light is injected orthogonally to the linear polarization of the solitary VCSEL. The dynamic behavior of the all-optical inverter under different pulsed optical inputs is analyzed. Time traces, rise and fall times of the linearly polarized output signals are reported. The dependence of these quantities on the bias current and injected optical power is investigated. This analysis permits us to identify proper operation conditions for all-optical inversion. The PS-based all-optical inverter is demonstrated with a 2.5 Gb/s non-return-to-zero (NRZ) input signal.**

***Index Terms*—All-optical switching/gating, all-optical signal processing, light polarization, polarization switching, optical injection, vertical-cavity surface-emitting lasers (VCSELs).**

I. Introduction

ALL-OPTICAL processing of high-speed signals is expected to be a key technology in future photonic networks. Of the range of candidate technological options semiconductor lasers have been shown to offer great promise [1-3]. Recently, the unique features of a special type of semiconductor laser, the vertical-cavity surface-emitting laser (VCSEL), has led to extensive research for its use in all-optical switching and signal processing [4-13]. VCSELs are very promising devices for these applications because of their small size, low power consumption, reduced fabrication costs, circular output beam, wafer level testing, ease of fabrication of 2D arrays, etc [4].

Optical injection in VCSELs has been a usual method to obtain nonlinear transfer functions useful for all-optical signal processing using those devices [4]. Those functions are obtained because optical injection strongly affects the transverse mode and polarization characteristics of VCSELs. On one hand optical injection can induce transverse mode switching in VCSELs. All-optical inversion [5-6] and signal regeneration [7] using transverse mode switching of a 1.55 μm VCSEL have been demonstrated. On the other hand optical injection can be used to obtain polarization switching (PS) of single transverse mode VCSELs. The optical polarization of a single transverse mode VCSEL has two possible orthogonal linear states. When the polarization of an injected optical field is orthogonal to that of the solitary VCSEL –the so called orthogonal optical injection- PS and bistability are observed [8-26]. PS by optical injection is expected to be fast and thus suitable for application in all-optical signal-processing systems. Based on this mechanism high-speed all-optical signal regeneration [8] and all-optical flip-flop memories [9-13] have been reported.

In this work we demonstrate all-optical inversion operation using the PS induced by orthogonal optical injection in a single-mode long-wavelength VCSEL. We consider low and high-frequency pulsed optical injection to describe the dynamic behavior of the all-optical inverter. Power time traces, as well as rise and fall times of each linear polarization are measured for different VCSEL bias currents and injected optical powers. We demonstrate all-optical inversion for NRZ signals at a bit rate of 2.5 Gb/s. These results offer exciting prospects for the use of PS in VCSELs in novel high-speed optical signal processing applications in present and future optical networks.

The paper is organized as follows. Section II gives a description of the experimental setup. In Sections III and IV we present results on the dynamic behavior of the all-optical inverter subject to a low-frequency periodic input. Sections III and IV focus on the dependence of the dynamics on the bias current and injected optical power, respectively. Section V is devoted to the analysis of the all-optical inverter subject to

Manuscript received October, 2011. This work has been funded in part by the Ministerio de Ciencia e Innovación, Spain, under project TEC2009-14581-C02-02 and by the the European Commission, under the Programme FP7 Marie Curie Intra-European Fellowships Grant PIEF-GA-2007-219682.

A. Quirce, J. R. Cuesta, A. Valle, and L. Pesquera are with the Instituto de Física de Cantabria, Consejo Superior de Investigaciones Científicas (CSIC)-Universidad de Cantabria, E-39005 Santander, Spain. A. Quirce is also with the Departamento de Física Moderna, Univ. de Cantabria, Facultad de Ciencias, E-39005, Santander, Spain (Phone: (+34) 942 201465. Fax: (+34) 942 200935. E-mail: quirce@ifca.unican.es; valle@ifca.unican.es; pesquerl@ifca.unican.es)

K. Schires, A. Hurtado, I. D. Henning and M. J. Adams are with the School of Computer Science and Electronic Engineering, University of Essex, Wivenhoe Park, CO4 3SQ, Colchester, U.K. (E-mail: krschi@essex.ac.uk; ahurt@essex.ac.uk; idhenn@essex.ac.uk; adamm@essex.ac.uk)

high-frequency NRZ input signals. Finally, in Section VI, discussion and conclusions are presented.

II. Experimental Setup

All-optical inversion operation is achieved using the experimental set-up shown in Fig. 1. An all-fiber system has been developed in order to inject the light from a tunable laser into a quantum-well commercially available 1550nm-VCSEL (RayCan^{TM}). The bias current and the temperature of the device were controlled with a laser driver and temperature controller, respectively. The temperature of the VCSEL was held constant at 298 ^{o}K for all the experiments. The polarization of the externally injected signal was controlled using fibre polarization controllers (PC). The injection of light into the VCSEL was obtained via a three-port optical circulator. A polarization controller (PC2) was used in order to inject linearly polarized light orthogonally to the linear polarization of the free-running VCSEL. An 85/15 fiber directional coupler was included in the setup to divide the optical signal from the tunable laser into two branches. The first branch was directly launched into the VCSEL, whilst the second one was connected to an Optical Multimeter (PM) to monitor the optical input power. The reflective output of the VCSEL was measured by connecting the third port of the optical circulator to an oscilloscope for the measurement of time traces. A polarization controller (PC3) and a polarization beam splitter (PBS) were included before the oscilloscope for the measurement of the time traces corresponding to each of the two linear polarizations of the VCSEL. An erbium doped fibre amplifier (EDFA) was also included in the final part of the setup to adjust the level of the reflective signal of the VCSEL for a proper measurement. Pulsed optical injection was obtained by using a Mach-Zender intensity modulator (MZM). The polarization of the light entering the MZM was controlled by a polarization controller (PC1). Electrical pulses generated by a 12.5 GHz pulse pattern generator (PPG) were amplified in a high-frequency amplifier and applied to the MZM for the modulation of the light coming from the tunable laser source.

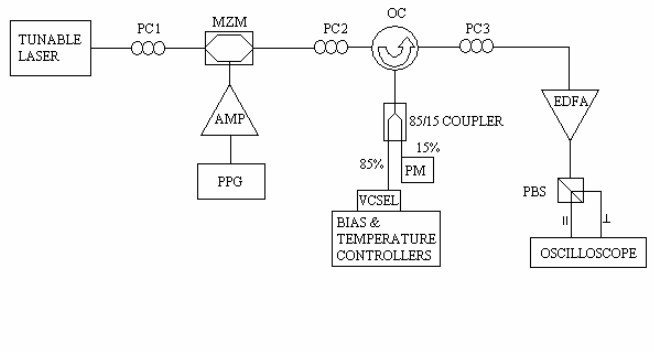

Fig. 1. Experimental set-up of all-optical inversion using the polarization switching in a VCSEL.

In the continuous wave (CW) regime the solitary VCSEL emits in the fundamental transverse mode with a threshold current of I_{th} = 1.9 mA, measured at the temperature of 298 K. We refer to the linear polarization of the light emitted by the VCSEL as "parallel" polarization. Fig. 2 shows that the lasing mode of the device with parallel polarization is located at the wavelength of 1550.98 nm when a bias current of 5 mA (I = 2.63 I_{th}) is applied to the VCSEL. The emission in that polarization is stable and no PS is observed for any bias current above threshold. The second subsidiary mode has orthogonal polarization appearing at 1551.47 nm wavelength. Fig. 2 shows that the orthogonal polarization is suppressed by 38 dB and it is shifted 0.49 nm to the long wavelength side of the lasing mode.

We have checked the detailed polarization mode of the main wavelength peak using the PBS at the output of the free-running mode VCSEL. We have measured the optical spectrum at each polarization output of the PBS and checked that the main wavelength peak only includes one polarization mode. We have also repeated the same measurements with another VCSEL of the same type (the one used in ref [25]) using a high-resolution (10 MHz) optical spectrum analyzer (BOSA) and checked that the main wavelength peak consists of a very narrow single peak corresponding to the parallel polarized fundamental mode.

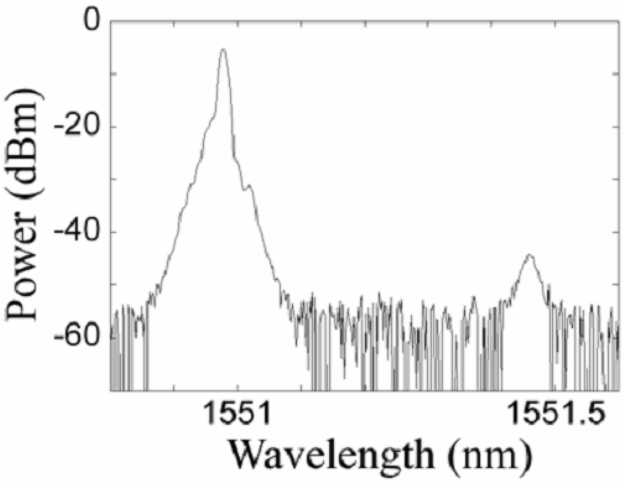

Fig. 2. Spectrum of the VCSEL biased with a current of 5 mA.

III. Dynamics under Low-Frequency Periodic Modulation: Effect of the Bias Current

The CW input-output power characteristics of the single-mode long-wavelength VCSEL subject to orthogonal optical injection have been recently measured [20],[23]. In these experiments the optical injection wavelength was near the wavelength of the orthogonal linear polarization. The output power of the parallel polarized optical signal as a function of the input power of the orthogonally polarized injected signal is illustrated in Fig. 5(d) of [20], and Fig. 3(a) of [23]. Both figures show the typical characteristics of all-optical inverters. When no external optical power is injected the output power of the parallel polarized mode is at a high or ON output state. If

the power of the orthogonal optical injection is increased, the parallel polarized output power gradually decreases until PS is obtained. At the PS point the power of the parallel polarized mode decreases abruptly from an ON to an OFF state. In this way an all-optical inverter based on PS in a VCSEL is obtained when considering the output power in the linear parallel polarization mode.

We have measured the dynamical response of this all-optical inverter using a pulsed optical input. Figs. 3 and 4 show the output power of the orthogonal and parallel polarized modes of the VCSEL when a squared-wave orthogonally polarized optical input is applied to the device. Results for two different values of bias current (3 and 5 mA) have been included in these figures. The wavelength detuning between the externally injected signal and the orthogonal polarization mode of the VCSEL, $\Delta\lambda$, is 0.05 nm. A low-frequency (50 MHz) periodic modulation has been used. The injected power arriving at the VCSEL under modulation conditions is $P_{inj} = 50$ μW.

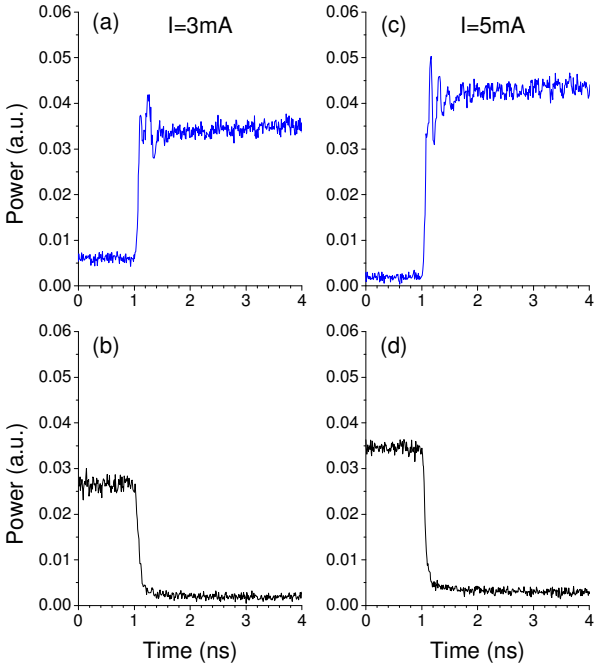

Fig. 3. Waveforms of the (a),(c) orthogonal and (b),(d) parallel polarizations during the rise of the optical input for two different bias currents: (a),(b) 3 mA, and (c),(d) 5 mA. In this figure $P_{inj} = 50$ μW.

Fig. 3 only shows the waveforms during the rise of the orthogonally polarized square-wave signal. Figs. 3 (a),(c) show the rise of the orthogonally polarized output of the VCSEL for applied bias currents of 3 and 5 mA, respectively. For the orthogonal polarized output, the squared shape of the optical input is reproduced with the exception of some small damped oscillations. Comparison between Figs. 3(a) and 3(c) shows that there is a small increase in the amplitude and frequency of the oscillations for larger bias currents.

The corresponding analysis for the parallel polarized output power is shown in Figs. 3(b),(d) for the two different applied bias currents. Figs. 3(b),(d) show a squared-shape response of the parallel polarized power during the rise of the orthogonally polarized input pulse. The parallel polarization output provides an inverted copy of the input signal. The abrupt decrease of the parallel polarized power coincides with the sharp increase of the orthogonally polarized power. No relaxation oscillations are observed during the decay of the parallel polarized power. Comparison between Figs. 3(a) and (c) (Figs. 3(b) and (d)) show that the rise time of the orthogonal (fall time of the parallel) polarized output pulses is rather similar for different bias currents.

The dynamical response of both linearly polarized modes during the fall of the orthogonally polarized input pulse is shown in Fig. 4. A large amplitude pulse appears in the orthogonally polarized output just after the fall of the optical input. Figs. 4(a),(c) show that the amplitude and width of this peak substantially increases with the bias current. The difference between the times at which that pulse appears and at which the orthogonal polarization begins to fall decreases as the bias current increases.

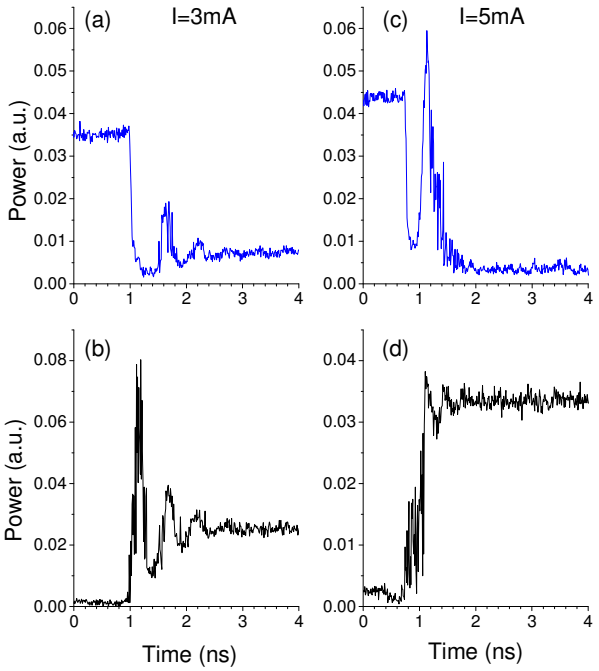

Fig. 4. Waveforms of the (a),(c) orthogonal and (b),(d) parallel polarizations during the fall of the optical input for two different bias currents: (a),(b) 3 mA, and (c),(d) 5 mA. In this figure $P_{inj} = 50$ μW.

The approach of the parallel polarized power to its steady state is characterized by damped oscillations as can be seen in Figs. 4(b),(d). The amplitude of the oscillations decreases as the bias current is increased. Figs. 4(a),(b) show that the frequencies of the oscillations of both linear polarizations are similar. As the bias current is increased the frequency of oscillations in the parallel polarization also increases. We have

checked that this frequency corresponds to the relaxation oscillation frequency of the solitary VCSEL. However, we have only observed several oscillations in the power of the orthogonal polarization when the bias current is 3mA. For larger values of the current only one peak is observed, as shown in Fig. 4(c). Figs. 4(b),(d) also show that the shape of the parallel polarized output approaches that of a step of increasing height as the bias current is increased. The height of the step increases linearly with the bias current as expected from the linear behavior of the L-I characteristics of the solitary VCSEL.

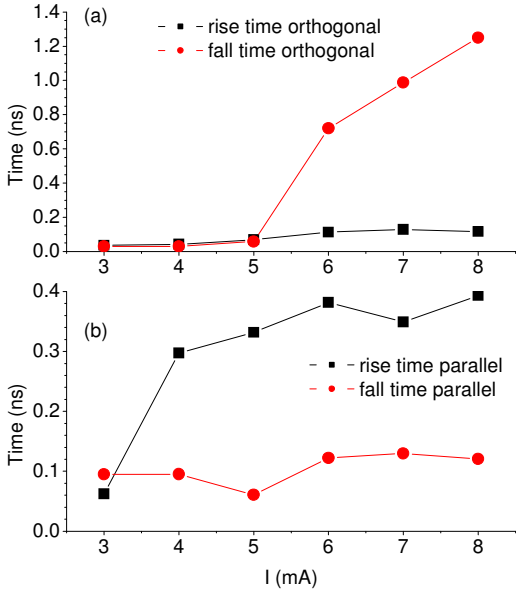

Fig. 5. Rise and fall times of the linear polarizations as a function of the bias current applied to the VCSEL: (a) Rise and fall times of the orthogonal polarization. (b) Rise and fall times of the parallel polarization. In this figure P_{inj} = 50 μW.

An analysis of the rise and fall times is desirable to complement the information given by Figs. 3 and 4. Fig. 5 shows the rise and fall times of both linearly polarized powers as a function of the applied bias current. We have measured the rise (fall) time as the time required for the power to change from a low to a high (high to a low) value near the steady-state. We have considered values of 20 and 80 % of the step height. Fig. 5 shows that the rise time of the orthogonal polarization and the fall time of the parallel polarization are very small. The rise time of the orthogonal polarization increases from 40 (I = 3mA) to 120 ps (I = 8mA). The fall time of the parallel polarization fluctuates at around 100 ps.

Fig. 5 also shows that the transition associated with the rise of the optical input (see Fig. 3) is faster than that associated with the fall of the optical input (see Fig. 4). The fall time of the orthogonal polarization increases to very large values due to the appearance of the large amplitude pulses of Figs. 4(a),(c). The rise time of the parallel polarization is very small (around 60 ps) for I = 3 mA. For larger bias currents that rise time increases to values between 300 and 400 ps. The fall time of the orthogonal polarization output is longer than the rise time of the parallel polarization only when I≥6 mA. When I is smaller (equal or larger) than 6 mA the 20 % level used to calculate the fall time of the orthogonal polarization is above (below) the first minimum that appears after switching-off this polarization. Then the longest time that is used to calculate the fall-time of the orthogonal polarization appears after the large spike when I≥6 mA. In this case the fall-time of the orthogonal polarization is much longer than the rise time of the parallel polarization because of the large value of the width of that spike.

IV. Dynamics under Low-Frequency Periodic Modulation: Effect of the Injected Power

In this section we measure the dynamical response of our system as a function of the injected optical power. A periodic modulation similar to that considered in section III is applied to the VCSEL. Figs. 6 and 7 show the output power of the orthogonal and parallel polarized modes when a 50 MHz squared-wave orthogonally polarized optical input is applied to the VCSEL. Results for two different values of P_{inj} (20 and 70 μW) have been included in those figures. A bias current of 5 mA has been chosen. In this way the cases analyzed in Figs. 3(c),(d) and Fig. 4(c),(d) are intermediate to those considered in Figs. 6 and 7, respectively.

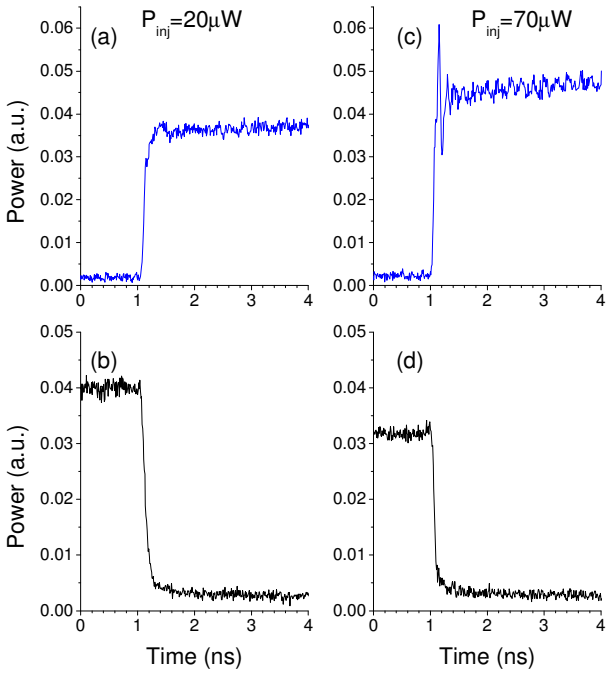

Fig. 6. Waveforms of the (a),(c) orthogonal and (b),(d) parallel polarizations during the rise of the optical input for two injected optical powers: (a),(b) 20 μW, and (c),(d) 70 μW. In this figure I = 5 mA.

Fig. 6 shows the waveforms during the rise of the orthogonally polarized input signal. The amplitude and frequency of the oscillations of the orthogonal polarized power increase when P_{inj} increases. The squared shape and the absence of relaxation oscillations during the fall of the parallel

polarized power is maintained throughout the whole P_{inj} range considered in this work.

Waveforms of both linearly polarized modes during the fall of the orthogonally polarized input pulse are shown in Fig. 7. Figs. 7(a),(c) show that the amplitude and width of the orthogonally polarized pulses slightly decrease as P_{inj} increases. Figs. 7(b),(d) and Fig. 4(d) show that the qualitative shape of the rise of parallel polarized power does not change significantly as P_{inj} is changed.

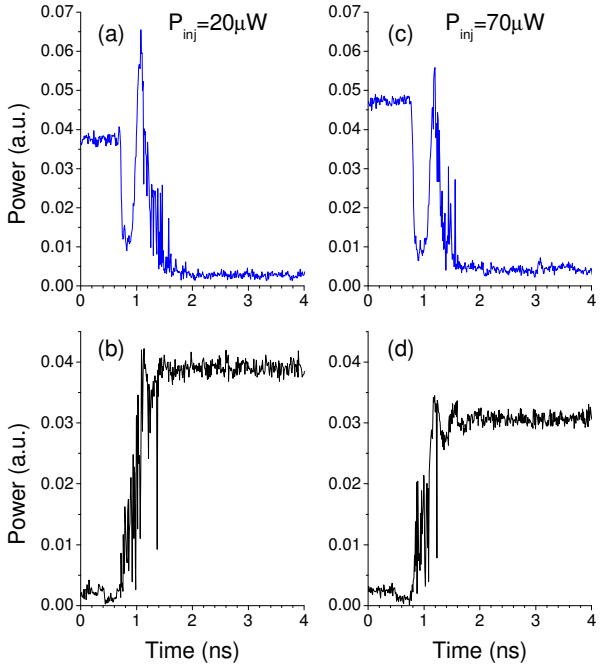

Fig. 7. Waveforms of the (a),(c) orthogonal and (b),(d) parallel polarizations during the fall of the optical input for two injected optical powers: (a),(b) 20 μW, and (c),(d) 70 μW. In this figure I = 5 mA.

The dependence of rise and fall times on P_{inj} is illustrated in Fig. 8. A slight decrease is observed for the rise and fall times as P_{inj} is increased. Due to our bias current choice (I = 5 mA) the numerical values for these times are small with the exception of the rise time of the parallel polarization (around 350 ps). In any case, these times are rather independent of the value of P_{inj}, at least for the range considered in this work. The measured values of rise and fall times for the parallel polarization indicate the potential of the PS-based all-optical inverter for operating at several Gb/s as will be shown in the next section.

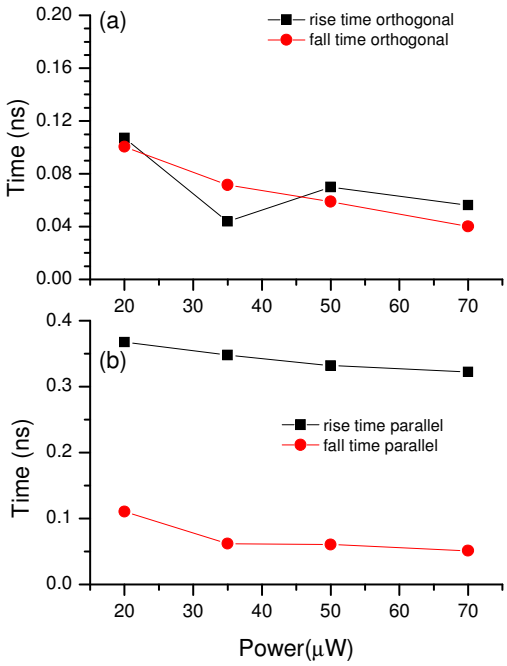

Fig. 8. Rise and fall times of the linear polarizations as a function of the injected optical power: (a) Rise and fall times of the orthogonal polarization. (b) Rise and fall times of the parallel polarization. In this figure I = 5 mA.

V. Dynamic Behavior Under High-Frequency Modulation

In this section we analyze the dynamic behavior of the all-optical inverter when subject to an optical input signal modulated at high-frequency. Fig. 9 shows results when a 2.5 Gbps NRZ optical signal with the following bit pattern "1011 1000 0111 0001 1110 1101 1010 0111" (a 32-bit word) is injected into the device. The wavelength detuning and optical input power are similar to those considered in the previous sections, $\Delta\lambda$ = 0.05 nm and P_{inj} = 50 μW. Typical rise and fall times (20-80 %) of the optical injection signal are 27 and 30 ps, respectively. The bias current applied to the VCSEL is 4 mA. Fig. 9(a) shows the input data arriving at the VCSEL's input. Fig. 9(b) shows the time response of the parallel polarized power, which is the output signal of the all-optical inverter. The comparison of Figs. 9(a) and 9(b) shows that good waveform inversion is experimentally demonstrated at 2.5 Gbps.

The power of the orthogonal polarization, shown in Fig. 9(c), presents some of the qualitative features already discussed in the previous sections. First, small damped oscillations appear during the build-up of the pulse. Second, large amplitude peaks, similar to those shown in Fig. 4 and Fig. 7, appear after the fall of the power of the orthogonal polarization. These unwanted spikes occur in the last "0" bit of "100" output bit sequences. These results suggest that use of the orthogonal polarization to obtain the all-optical gating functionality would suffer from pattern-dependent error-rate degradation.

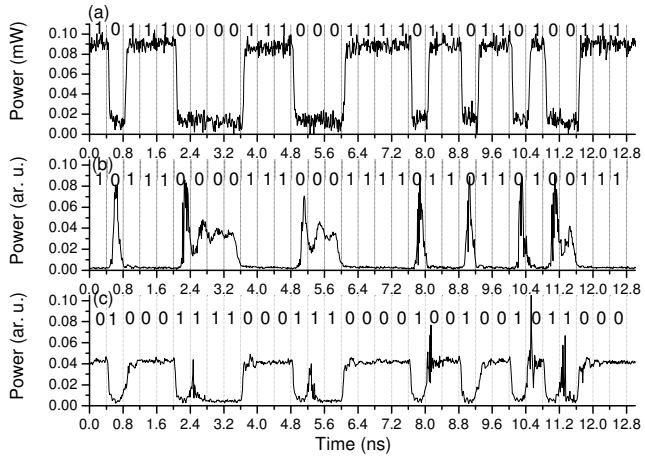

Fig. 9. Waveform inversion of a 2.5 Gb/s NRZ input signal. (a) Input light. (b) Power of the parallel polarization. (c) Power of the orthogonal polarization. The VCSEL is biased at 4 mA.

VI. Discussion & Conclusions

The detailed polarization properties of VCSELs varies from chip to chip even though they are all single-mode VCSELs made from the same wafer. We have repeated the same measurements with another VCSEL of the same type (the one used in ref. [25]) to see whether the strong pulse spike that appears in the orthogonal polarization direction after turn-off of the injection pulse is observed or not. Results are shown in Fig. 10. Fig. 10(a) and Fig. 10(b) show the waveforms of the orthogonal polarization during the fall of the optical input for two different bias currents.

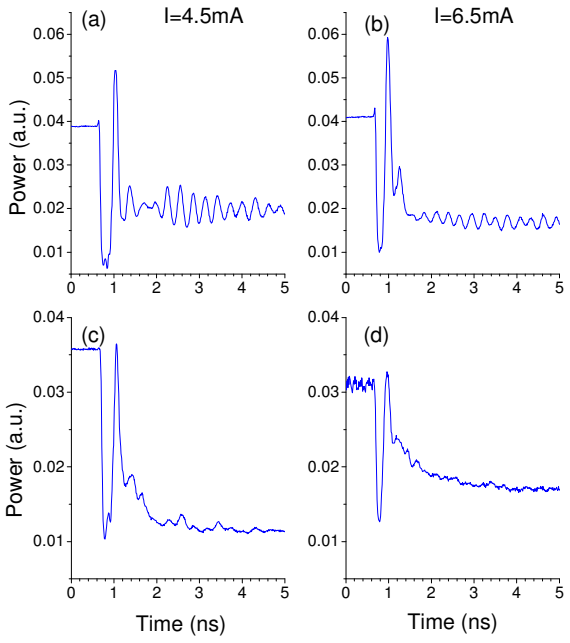

Fig. 10. Waveforms of the orthogonal polarizations during the fall of the optical input for a different VCSEL. (a) $\Delta\lambda$=0.05 nm, I=4.5 mA ; (b) $\Delta\lambda$=0.05 nm, I=6.5 mA; (c) $\Delta\lambda$=0 nm, I=4.5 mA; (d) $\Delta\lambda$=0 nm, I=6.5 mA. In this figure P_{inj} = 50 μW.

The same phenomenon is observed: a strong spike appears just after the fall of the optical input. The amplitude of the spike increases with the bias current as shown by comparing Fig. 10(a) and Fig. 10(b). Using this VCSEL we have made also measurements for a different detuned wavelength. Fig. 10(c) and Fig 10(d) shows the results for $\Delta\lambda$=0 nm and two different bias currents. Strong spikes keep on appearing. The width of the spike increases with the bias current. The amplitude of the spikes is smaller than those obtained for $\Delta\lambda$=0.05 nm.

Optical inversion of the same type of VCSEL has also been reported in [26]. In their experiment two injected beams are required for optical inversion: first, a CW light is injected into the orthogonal polarization, then another parallel polarized pulsed optical injection is injected near the wavelength corresponding to the parallel polarization. The injection locked orthogonal polarization mode acts as the output of the inverter. Our experiment is different because only one injected beam is required for optical inversion: an orthogonal polarized pulsed optical injection is injected near the wavelength corresponding to the orthogonal polarization. In this way the parallel polarization mode is the one acting as the output of the inverter.

The relevant quantity for the evaluation of the dynamic characteristics of the PS-based all-optical inverter is the corresponding time dependence of the parallel polarized output. Experimental results of Fig. 5 and Fig. 8 show that the rise time of the parallel polarized power is much larger than the fall time of that polarization: typical values of that rise (fall) time are between 0.3 and 0.4 ns (around 0.1 ns). This suggests that the operation speed of the all-optical inverter is limited by the rising edges of parallel polarized pulses. A possibility to avoid that limitation is to consider small bias current values: Fig.5 shows that the rise time of the parallel polarization is an increasing function of the bias current. In fact, values of that rise time can be much smaller than 0.1 ns for a 3 mA bias current. However, the advantages of a small rise time are overshadowed by the small extinction ratio for the parallel polarized power obtained in that case. An increase of the injected optical power does not seem to solve this problem either because Fig. 8 shows that the rise time decreases very slowly with P_{inj}. Nevertheless, our results show that all-optical inversion can be obtained with a 2.5 Gb/s NRZ input signal with a particular 32-bit word modulation. It would be interesting to extend our analysis to a high-frequency pseudorandom word modulation in order to know the impact of different words on the BER of the system.

The orthogonal polarization output shows unwanted spikes that degrade the response of the system for all-optical gating operation. These spikes keep on appearing when a 2.5 Gbs NRZ input signal is considered. These results suggest that the use of orthogonal polarization to obtain all-optical gating would suffer from pattern-dependent error-rate degradation. These findings require further investigation to determine under which conditions all-optical gating could be successfully

obtained with a VCSEL in conjunction with all-optical inversion operation.

Our experiments show that all-optical inversion is obtained at an operation speed of 2.5 Gbps with a commercially available device without any further device design optimization. A big advantage of all-optical switching operation is the speed which cannot be matched by electrical modulation. The resonant injection field can perturb the cavity field directly. The switching speed is mostly limited by the injection pulse speed. Finally, we should also note that our experiments were carried out with a device emitting at 1550 nm, the most used wavelength in long-haul optical networks, offering promise for novel uses of VCSELs in present and future optical telecommunication networks.

Summarizing, we have experimentally demonstrated all-optical inversion using PS of a long-wavelength single-mode VCSEL. The dynamic behavior of the all-optical inverter under low and high-frequency optical inputs has been analyzed. Time traces, rise and fall times of the linearly polarized output signals have been measured. The dependence of these quantities on the bias current applied to the VCSEL and on the injected optical power has been investigated. The PS-based all-optical inverter has been demonstrated with a 2.5 Gb/s NRZ input signal. These results show that polarization switching in VCSELs can be a useful mechanism for high-speed optical signal processing applications.

ACKNOWLEDGEMENT

The authors would like to thank Dr. Georgios Zervas and Prof. Dimitra Simeonidou from the University of Essex for lending the oscilloscope and pulse pattern generator used in this work.

REFERENCES

[1] H. Kawaguchi, "Bistability and nonlinearities in laser diodes," Norwood, MA. Artech House (1994).

[2] H. Kawaguchi, "Bistable laser diodes and their applications", *IEEE J. Select. Topics Quantum Electron*., vol. 3, no. 5, pp.1254-1270, Oct. 1997.

[3] M. J. Adams, A. Hurtado, D. Labukhin, and I. D. Henning, "Nonlinear semiconductor lasers and amplifiers for all-optical information processing", *Chaos*, vol. 20, art. 037102, 2010.

[4] F. Koyama, "Recent advances of VCSEL Photonics," *J. Lightwave Technol.* vol. 24, no. 12, pp. 4502-4513, Dec. 2006.

[5] Y. Onishi, N. Nishiyama, C. Caneau, F. Koyama, and C.E. Zah, "All-optical inverter based on long-wavelength vertical-cavity surface-emitting laser," *IEEE J. Select. Topics Quantum Electron*., vol. 11, no. 5, pp. 999-1005, Sep./Oct. 2005.

[6] Y. Onishi, N. Nishiyama, C. Caneau, F. Koyama, and C.E. Zah, "Dynamic behavior of an all-optical inverter using transverse-mode switching in 1.55 microns vertical-cavity surface-emitting lasers", *IEEE Photon. Technol. Lett.,* vol.16, no. 5, pp. 1236-1238, May 2004.

[7] Y. Onishi, and F. Koyama, "All-optical regeneration using a vertical-cavity surface-emitting laser with external light injection," *IEICE Trans. Electron.,* vol. E87C, no. 3, pp. 409-415, Mar. 2004.

[8] T. Mori, Y. Sato, and H. Kawaguchi, "Timing jitter reduction by all-optical signal regeneration using a polarization bistable VCSEL", *J. Lightwave Technol*. vol. 26, no. 16, pp. 2946-2953, Aug. 2008.

[9] T. Mori, Y. Yamayoshi and H. Kawaguchi, "Low-switching-energy and high-repetition-frequency all-optical flip-flop operations of a polarization bistable vertical-cavity surface-emitting laser," *Appl. Phys. Lett*., vol. 88, no. 10, 101102, Mar. 2006.

[10] J. Sakaguchi, T. Katayama, and H. Kawaguchi, "All-optical memory operation of 980-nm polarization bistable VCSEL for 20-Gb/s PRBS RZ and 40-Gb/s NRZ data signals," *Opt. Exp.,*vol. 18, no. 12, pp. 12362-12370, Jun. 2010.

[11] J. Sakaguchi, T. Katayama, and H. Kawaguchi, "High switching-speed operation of optical memory based on polarization bistable vertical-cavity surface-emitting laser," *IEEE J. Quantum Electron*., vol. 46, no. 11, pp. 1526-1534, Nov. 2010.

[12] S. H. Lee, H. W. Jung, K. H. Kim, M. H. Lee, B. S. Yoo, J. Roh, and K. A. Shore, "1-GHz all-optical flip-flop operation of conventional cylindrical-shaped single-mode VCSELs under low-power optical injection", *IEEE Photon. Technol. Lett.,* vol. 22, no. 23, pp. 1759-1761, Dec. 2010.

[13] S. H. Lee, H. W. Jung, K. H. Kim, and M. H. Lee, "All-optical flip-flop operation based on polarization bistability of conventional 1.55-μm wavelength single-mode VCSELs", *J. Opt. Soc. Korea*, vol. 14, no. 2, pp. 137-141, Jun. 2010.

[14] Z. G. Pan, S. Jiang, M. Dagenais, R. A. Morgan, K. Kojima, M. T. Asom, and R. E. Leibenguth, "Optical injection induced polarization bistability in vertical-cavity surface-emitting lasers," *Appl. Phys. Lett*., vol. 63, no. 22, pp. 2999-3001, Nov.1993.

[15] D. L. Boiko, G. M. Stephan and P. Besnard, "Fast polarization switching with memory effect in a vertical cavity surface emitting laser subject to modulated optical injection," *Journal of Applied Physics,* vol. 86, no. 8, pp. 4096-4099, Oct.1999.

[16] Y. Hong, K. A. Shore, A. Larsson, M. Ghisoni and J. Halonen, "Pure frequency-polarisation bistability in vertical-cavity surface-emitting lasers subject to optical injection," *Electron. Lett.,* vol. 36, no. 24, pp. 2019-2020, Nov. 2000.

[17] B. S. Ryvkin, K. Panajotov, E. A. Avrutin, I. Veretennicoff and H. Thienpont, "Optical-injection-induced polarization switching in polarization-bistable vertical-cavity surface-emitting lasers," *J. Appl. Phys.*, vol. 96, no. 11, pp.6002-6007, Dec. 2004.

[18] M. Sciamanna and K. Panajotov, "Route to polarization switching induced by optical-injection in vertical-cavity surface-emitting lasers", *Phys. Rev. A*, vol. 73, no. 2, 023811, Feb. 2006.

[19] J. Buesa, I. Gatare, K. Panajotov, H. Thienpont and M. Sciamanna, "Mapping of the dynamics induced by orthogonal optical injection in vertical-cavity surface-emitting laser," *IEEE J. Quantum Electron*., vol. 42, no. 2, pp. 198-207, Feb. 2006.

[20] A. Hurtado, I. D. Henning, and M. J. Adams, "Two-wavelength switching with a 1550 nm VCSEL under single orthogonal optical injection," *IEEE J. Sel. Top. in Quantum Electron*, vol. 14, no. 3, pp. 911-917, May/Jun.2008.

[21] A. Valle, M. Gomez-Molina, and L. Pesquera, "Polarization bistability in 1550 nm wavelength single-mode vertical-cavity surface-emitting lasers subject to orthogonal optical injection," *IEEE J. Sel. Top in Quantum Electron.*, vol. 14, no. 3, pp. 895-902, May/Jun.2008.

[22] K. H. Jeong, K. H. Kim, S. H. Lee, M. H. Lee, B. S. Yoo and K. A. Shore, "Optical injection-induced polarization switching dynamics in 1.5 mu m wavelength single-mode vertical-cavity surface-emitting lasers," *IEEE Photon. Technol. Lett.,* vol. 20, no. 9-12, pp. 779-781, May. 2008.

[23] A. Hurtado, A. Quirce, A. Valle, L. Pesquera, and M. J. Adams, "Power and wavelength polarization bistability with very wide hysteresis cycles in a 1550nm-VCSEL subject to orthogonal optical injection", *Opt. Exp*., vol. 17, no. 26, pp. 23637-23642, 2009.

[24] M. S. Torre, A. Hurtado, A. Quirce, A. Valle, L. Pesquera, and M. J. Adams, "Polarization switching in long-wavelength VCSELs subject to orthogonal optical injection", *IEEE J. Quantum Electron*, vol. 47, no. 1, pp. 92-99, 2011.

[25] A. Hurtado, A. Quirce, A. Valle, L. Pesquera, and M. J. Adams, "Nonlinear dynamics induced by parallel and orthogonal optical injection in 1550 nm vertical-cavity surface-emitting lasers (VCSELs)", *Opt. Exp*., vol. 18, no. 9, pp. 9423-9428, 2010.

[26] C. F. Marki, S. Moro, D. R. Jorgesen, P. Wen, and S.C. Esener, "Cascadable optical inversion using 1550 nm VCSEL", *Electron. Lett*., vol. 44, no. 4 , pp. 292-293, Feb. 2008.

A. Quirce received the Licenciada en Física (Ms. Sc.) degree from the Universidad de Cantabria, Spain, in 2008. She is currently working toward the PhD degree in Physics. Her current research interests are in the areas of

dynamics of vertical-cavity surface-emitting lasers and optical injection effects in semiconductor lasers.

J. R. Cuesta received the Licenciado en Física (Ms. Sc.) degree from the Universidad de Cantabria, Spain, in 2010.

K. Schires received the Diplôme d'Ingénieur degree, specializing in signal processing and telecommunications, from the École Supérieure d´Ingénieurs en Électronique et Électrotechnique, Paris, France, in 2008. He is currently working toward the Ph.D. degree in semiconductor electronics with the School of Computer Science and Electronic Engineering, University of Essex, Colchester, UK.

A. Hurtado was born in Madrid, Spain, in 1976. He received the Graduate degree in Telecommunications Engineering from the E.T.S. Ingenieros de Telecomunicación, Universidad Politécnica de Madrid, Spain, in 2001, and the PhD degree in Photonic Technology from the Universidad Politécnica de Madrid, in 2006.

Since 2007 he has been with the Optoelectronics Research Group of the University of Essex (UK) where he works as a Research Fellow. He has been awarded with two Marie Curie Fellowships by the European Commision (calls 2007 and 2010). His current research interests include semiconductor lasers and amplifiers, optical injection, laser's nonlinear dynamics, bistability and optical switching devices.

A. Valle was born in Reinosa, Cantabria, Spain, in 1965. He received the M. Sc. and Ph.D. degree in physics from the Universidad de Cantabria, Spain, in 1988 and 1993, respectively.

During 1994 and 1995, he was a postdoctoral fellow at the School of Electronic and Electrical Engineering at the University of Bath, England. In 1996 he joined the Instituto de Física de Cantabria (CSIC-UC). Since 1998 he has been lecturer at the Departamento de Física Moderna at the University of Cantabria, Spain. His research interests are in the areas of vertical-cavity surface-emitting lasers, noise and nonlinear dynamics of semiconductor lasers.

L. Pesquera was born in Vega de Infanzones, León, Spain, in 1952. He received the M.Sc. degree in physics in 1974 from the Universidad de Valladolid, Spain. He was a postgraduate fellow at the Université de Paris VI during 1977-1980. He received the Ph.D. degree in physics in 1980 from the Universidad de Cantabria, Santander, Spain.

In 1980 he joined the Departamento de Física Moderna of the Universidad de Cantabria. Since 1991 he has been Professor of Physics at the Universidad de Cantabria. In 1995 he joined the Instituto de Física de Cantabria (CSIC-UC). His research work started in the field of stochastic processes applied to Physics and he has made contributions to the foundations of quantum physics, fluctuations in nuclear reactors, disordered systems and laser physics. He is currently working on the modeling of noise and nonlinear properties of semiconductor lasers and their applications to optical communication systems.

Ian D Henning graduated with First Class Honors in Applied Physics from the University of Wales, Cardiff, U.K., in 1976 and the Ph. D. degree studying deep levels GaAsP, which was done in collaboration with General Electric Company, Hirst Research Centre, Wembley, U.K.

In 1980, he joined the Devices Division Telecoms Research Laboratories at Martlesham Heath, where he specialized in theory and measurements of semiconductor lasers. He led work on integrated semiconductor optoelectronics devices and then the photonic integrated circuits, as well as on developing a novel optical microwave devices activity. In February 2002, he joined the Department of Electrical Sytems Engineering, Essex University, Colchester, U.K., as a Professor. He has authored or co-authored more than 80 papers published in refereed journals, holds ten patents, and has co-authored two books.

Dr. Henning is a Fellow of the Institution of Electrical Engineering and the Institute of Physics.

M. Adams received the Ph.D. degree in laser theory from the University of Wales, Cardiff, U.K., in 1970. He was engaged in optoelectronics research and development with 15 years experience in industry (Plessey, BT), and 26 years in academia (University of Cardiff, University of Southampton, University of Essex, Colchester, U.K.). Since 1996, he has been a Professor at the University of Essex. His current research interests include semiconductor lasers, optical amplifiers, optical waveguides, optical bistability, semiconductor nonlinear optics and optical switching devices, and nonlinear dynamics of lasers. He is the author or co-author of many articles published widely in the optoelectronics field over many years, including a standard text on optical waveguide theory and two books in semiconductor lasers and optical fibers for use in telecommunications.